INTERNATIONAL JOURNAL OF AUTOMOTIVE AND MECHANICAL ENGINEERING (IJAME)
ISSN: 2229-8649 e-ISSN: 2180-1606
VOL. 19, ISSUE 3, 9964 – 9970
DOI: https://doi.org/10.15282/ijame.19.3.2022.08.0768

ORIGINAL ARTICLE

Effect of Polytetrafluoroethylene Binder Content on Gravimetric Capacitance and Life Cycle Stability of Graphene Supercapacitor

R.N.A.R. Seman[1], M.A. Azam[1,*], M.A. Mohamed[2] and M.H. Ani[3]

[1]Fakulti Kejuruteraan Pembuatan, Universiti Teknikal Malaysia Melaka, Hang Tuah Jaya, 76100 Durian Tunggal, Melaka, Malaysia.
[2]Institute of Microengineering and Nanoelectronics, Universiti Kebangsaan Malaysia, 43100 Bangi, Selangor, Malaysia.
[3]Faculty of Engineering, International Islamic University Malaysia, 50728 Kuala Lumpur, Malaysia.

ABSTRACT – One of the major elements in determining the supercapacitor performance is the development of a nano-layered structure through facilitating the surface-dependent electrochemical reaction processes. Carbon-based nanomaterials especially graphene, has attracted tremendous interest in electrical charge and power sources including supercapacitor because of their exceptional properties, which include high conductivity and large specific surface area. In this paper, the effect of polytetrafluoroethylene (PTFE) binder ratio (1, 5, 10, and 15 wt. %) on the electrochemical performance of graphene supercapacitor are evaluated. In addition, the facile and scalable preparation of graphene electrodes by using low-cost slurry technique is proposed. From the conducted experimental works, it was found that the fabricated graphene electrodes exhibit superior electrochemical properties for supercapacitor applications with a specific gravimetric capacitance of up to 373 F g−1. Moreover, the graphene electrode presented excellent cyclic stability with 99 % specific capacitance retention after 10,000 charge/discharge cycles hence promising for long-lasting supercapacitors. The outcomes from the deliberated study serve as the basis of knowledge in the development of a cost-effective graphene-based materials production for energy storage devices.

ARTICLE HISTORY
Received: 12th Sept 2021
Revised: 29th June 2022
Accepted: 19th Sept 2022
Published: 30th Sept 2022

KEYWORDS
PTFE binder; Graphene supercapacitor; 6M KOH electrolyte; Electrochemical performance

INTRODUCTION

The energy supply is estimated to keep increasing due to global environmental issues, global economy, and air pollution. The challenges that scientists and researchers are facing today are to develop new materials for efficient energy conversion and storage hence providing a low cost and environmentally friendly for communities and societies [1-3]. Several efforts have been made to create advanced materials for high performance energy storage devices, including fuel cells, batteries and supercapacitors. Nowadays, Supercapacitors are largely employed in several uses as mobile electronics and hybrid electric vehicles owing to their lightweight, long life cycles, high rate performance, high specific energy and power densities [4-6].

Supercapacitors have been used in computer memory backup power since their first commercialization in the market in the past decades [7]. The majority of about 95% of the commercialized supercapacitors had utilized carbon-based materials as electrodes in the systems [8]. Based on the charge storing mechanism, supercapacitors are primarily divided into two types. The electric double-layer capacitor (EDLC) is reigned by ion electrosorption at the electrode surface for storing energy. Meanwhile, pseudocapacitor is based on the Faradaic charge transfer [9]. Also, nickel foam has been selectively used as a current collector for the electrode in the supercapacitor. Generally, due to the porous nature of nickel backbone and the effectiveness of nickel foam as an electrically conductive substrate which possesses exceptional mechanical strength and makes it easy for the electrolyte to enter in the electrochemical cell for the transmission of charges.

Conventionally, the electrodes are prepared by mixing and stirring the active materials, conductive agents and binders together to form a homogeneous slurry before being coated onto the current collector. In order to avoid the active electrode falling down during the testing, the binder was used to bind the active material and conductive agent. Various binders have been used to fabricate the supercapacitor electrode materials, including poly(tetrafluoroethylene) (PTFE), nafion, and poly(vinylidenedifluoride) (PVDF) [10]. Although PTFE has been the best choice for supercapacitor binder material, PTFE is known for its insulative property and exhibits hydrophobicity to the electrolyte. These features enhance internal resistance and reduce the effectiveness of the active material [11-13]. Thus, there is need to experimentally explore more about this binder material. Nafion shows excellent hydrophilicity with good chemical stability, however, the cost/price remains the major drawback in large-scale supercapacitor fabrication [14,15]. Meanwhile, the PVDF demonstrates unique polarity and excellent swelling property in the electrolyte, however, it is hardly to be homogeneous during the slurry mixing process [16,17].

The objective of this study is to compare the functionality of graphene electrode materials based on various PTFE binder formulations. This paper presents a facile solid-state technique to prepare graphene electrode for supercapacitor.

*CORRESPONDING AUTHOR | M.A. Azam | ✉ asyadi@utem.edu.my

Various binder compositions of 1, 5, 10 and 15 wt. % were employed to compare the electrochemical performance and to choose the optimized ratio for PTFE binder in the supercapacitor.

EXPERIMENTAL

Preparation of Graphene Electrode

The compositions listed in Table 1 provide the foundation for the preparation of graphene electrodes. Firstly, electrode materials were made by agitating the required amounts of graphene that had been purchased (Sigma Aldrich), super-P (TIMCAL) and PTFE to form uniform slurries. The slurries were then scraped onto nickel foam sheets (15 mm in diameter). Finally, the resultant working electrodes were then pressed at 3000 Psi and dried in a circulating oven at 60 °C for 12 h. Meanwhile, the electrochemical experiments were conducted in a three-electrode cell with Pt and Ag/AgCl serving as the counter and reference electrodes, respectively, and a 6 M potassium hydroxide (KOH) solution as the electrolyte. The average active material mass loading was kept between 0.5 and 2.0 mg.

Table 1. Slurry composition of graphene supercapacitor electrode.

Sample name	Ratio (Graphene:Super-P:PTFE)
Sample 1 (S1)	89:10:1
Sample 2 (S2)	85:10:5
Sample 3 (S3)	80:10:10
Sample 4 (S4)	75:10:15

Characterization of Graphene Electrode

Raman spectroscopy was used to examine the structural characteristics of the graphene electrode at = 532 nm within the 500 cm^{-1} to 3000 cm^{-1} Raman shift range. To confirm the crystal structure and phase, XRD analysis (Bruker PANalytical, Cu Kα radiation, λ = 0.15406 nm) was employed. The morphology of the electrode material was examined using field emission scanning electron microscopy (FESEM; Hitachi, SU8000, 2.0 kV).

Electrochemical Measurement of Graphene Electrode

The cyclic voltammetry (CV) and galvanostatic charge-discharge (GCD) measurements were performed by WonAtech electrochemical workstation. The CV measurements were carried out from 0.5 V to 1.0 V at the scan rates of 1, 5, 10, 20, 40, 50, 60, 80, 100 mV s^{-1}. Meanwhile, GCD investigation was carried out from 0.5 to 1.0 V at the current of 1, 5, 10 and 15 mA which is equivalent to 0.5, 2.5, 5.0 and 7.5 A g^{-1} current densities (calculated from 2.0 mg average mass). The specific gravimetric capacitances, C_{sp} were calculated according to Eq. (1) and (2) [18] :

$$\boldsymbol{Csp} = \int_{E1}^{E2} i\ (E)dE\ \div (E2 - E1)mv \tag{1}$$

where *E1* and *E2* are CV's cut-off potentials, cyclic voltammetry current is denoted by *i(E)*, $\int_{E1}^{E2} i\ (E)dE$ is the total charges determined by integrating the charge and discharge sweeps in a CV, *(E2-E1)* is the chosen possible voltage width, *m* is the average measure of the weight of electrode material, and *v* is the voltage range of scanning segments. The equation for specific gravimetric capacitance calculated from the GCD curves is as follows:

$$\boldsymbol{Csp} = 2I/(m\ (dV/dt)) \tag{2}$$

where *I* is current, m stands for the average electrode mass. and *dV/dt* is the discharge curve's slope following the voltage (IR) drop. The CV and GCD measurements were conducted on WonAtech electrochemical workstation of the three-electrode setup in the aqueous-based solution.

EXPERIMENTAL RESULTS

Structural and Morphological Properties of Graphene Electrode

Figure 1(a) illustrates the Raman spectrum for the graphene electrodes using PTFE as the binder. In theory, the defect level in sp^2-bonded carbon atom domains can be determined using the Raman relative peak intensity or area ratio of the D to G band (I_D/I_G) [19]. Raman spectrum showed the D and G bands at 1344 cm^{-1} and 1599 cm^{-1}, respectively, with an I_D/I_G ratio of 0.84. Typically, the D peak at 1344 cm^{-1} from the degree of defect in graphene is described by the double resonance process. (sp^3-hybridized carbon). The remarkable suppressed D band indicates less defects and good quality of graphene material, while the G band is created by the first-order scattering of E_{12g} phonon and represents the E_{12g} zone centre mode of the crystalline graphite. The layer amount of graphene was often described using the ratio of 2D and G peaks' integrated intensities (I_{2D}/I_G). The I_{2D}/I_G ratio is 1.74 in which the graphene consists of a few layer structure. The result obtained from Raman spectroscopy analysis shows the existence of graphene.

The phase identification of graphene electrode coated on the Ni foam substrate was conducted by using XRD (Figure 1(b)). The graphene peak (002) does not exist due to the thin layer of graphene on the surface of Ni foam. The observed peaks, 43.42 (002), 52 (200), and 77 (200), are caused by the presence of Ni phase in the substrate or current collector. The microstructures and morphologies of graphene were examined using the FESEM technique (Figure 1(c)). The graphene FESEM image shows a micrometre-scale rippled morphology of the typical graphene layer sheet. FESEM image of graphene sheets, illustrating the uniformly distributed of graphene layers onto the Ni foam.

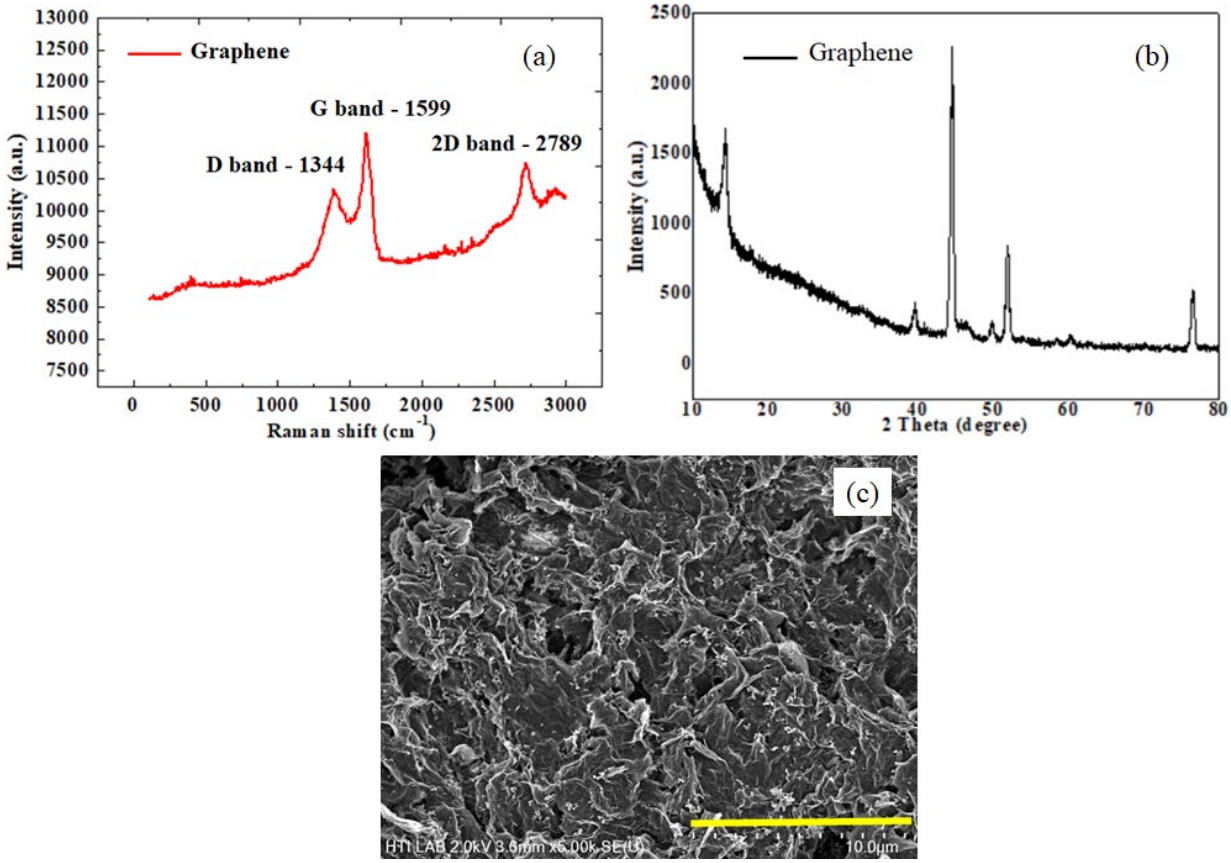

Figure 1. Characterization of graphene electrode on Ni foam. (a) Raman spectrum, (b) XRD pattern, and (c) FESEM image.

Cyclic Voltammetry

The CV curves of graphene with different ratio at scan rate of 1 to 100 mV s^{-1} are presented in Figure 2. It is exhibited in a rectangular shape that it is typical of an electrical double-layer material at a high scan rate of 100 mV s^{-1} showing a superior electric double-layer capacitance (EDLC) behavior and minimal contact resistance [20-22]. This is due to the fact that graphene atomic structures store electrical charges by using an adsorption-desorption mechanism. Commonly, the calculated curve area is critical to determine the C_{sp} values. Sample 4 (313.95 F g^{-1}) clearly exhibits the highest C_{sp} among the other samples, followed by Samples 3 (135.88 F g^{-1}), Sample 2 (135.88 F g^{-1}), and Sample 1 (135.88 F g^{-1}), respectively. According to earlier research, 15% of PTFE ratio is suggested to be reasonable to bind with graphene [23]. Also, it was discovered that the paste could not be tightly bound when the PTFE to graphene ratio reduced to a certain amount. The CV data demonstrate the patterns in capacitance fluctuation as PTFE content rises. The capacitance values increase linearly from 74.87 to 313.95 F g^{-1} when the PTFE content is reduced from 15 to 1 wt%. It makes sense, given that less-isolated PTFE would block less of the active region and have better conductivity [24]. These values were further tabulated in Table 2.

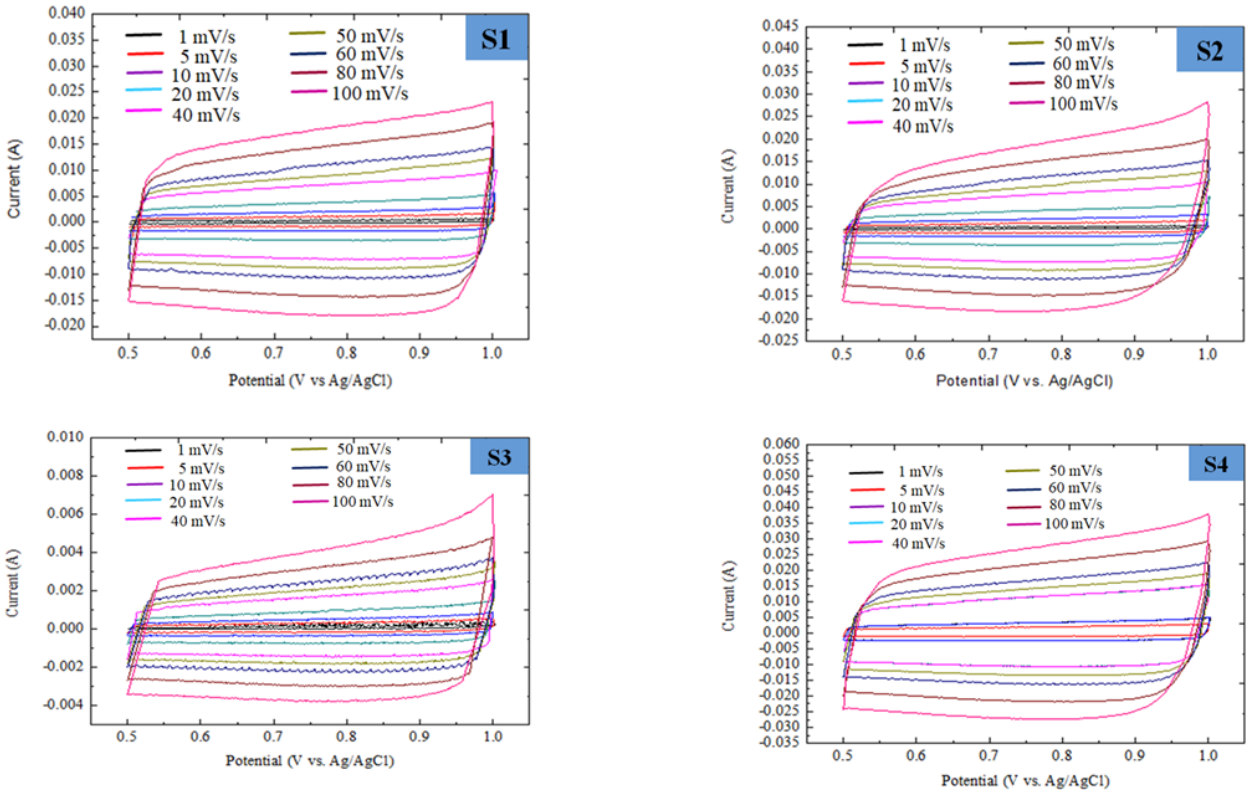

Figure 2. Recorded CV results in a potential range of 0.5-1.0 V at different scan rates in 6 M KOH electrolyte.

Galvanostatic Charge-Discharge

Figure 3 shows the galvanostatic charge-discharge (GCD) curves of graphene electrodes which were performed at different currents of 1, 5, 10, and 15 mA. It was found that the charge and discharge curves of all samples are almost linear with symmetrically constant slopes indicating the excellent capacitive behaviour of the graphene electrodes [20]. The charge and discharge curves are all approximately symmetrical triangular shapes with currents between 1 and 15 mA. This suggests that S1, S2, S3 and S4 possess excellent electrochemical reversibility [25]. In addition, all samples exhibit good rate performance showing nearly straight lines of GCD curves. These demonstrate the usual capacitive behaviour of EDLC-type supercapacitors [26]. Remarkably, S4 retains a high capacitance value of 373 F g^{-1} even at a high current density of 7.5 A g^{-1}.

The most crucial factor in determining the lifespan of electrode materials for real supercapacitor applications is cycling stability. The classification of supercapacitors' cyclic stability is based on their ability to maintain nearly 100% after an extended cycle. Figure 4 shows the variation of capacitance retention with the function of cycle number for the graphene electrode. As a result, the graphs were labelled with different colours. The electrochemical stability of the graphene electrode was evaluated through the 10,000 cycles of charge and discharge at the current of 35 mA, equivalent to 17.5 A g^{-1} current density. The capacitance retention of S1, S2, S3, and S4 are 99, 97, 96 and 94 %, respectively, after 10,000 cycles. Overall, all electrodes exhibit high capacitance retention at a minimum of 94 %, suggesting high charge transfer efficiency throughout the 10,000 cycles, excellent cycling stability and an extremely low fade rate at high current and reversibility of the charge/discharge processes [27, 28]. This may be because of the graphene electrode's structural stability and strong ion diffusion [29].

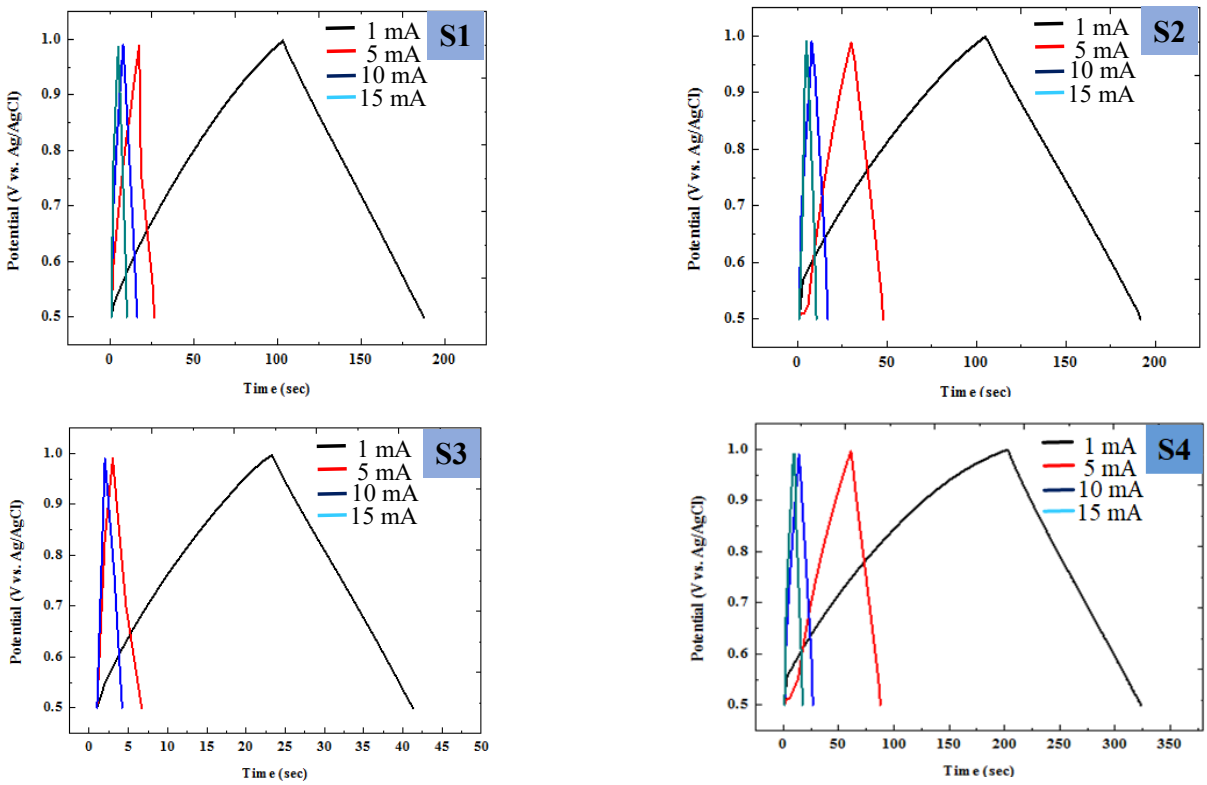

Figure 3. GCD curves at different currents for all composition ratios.

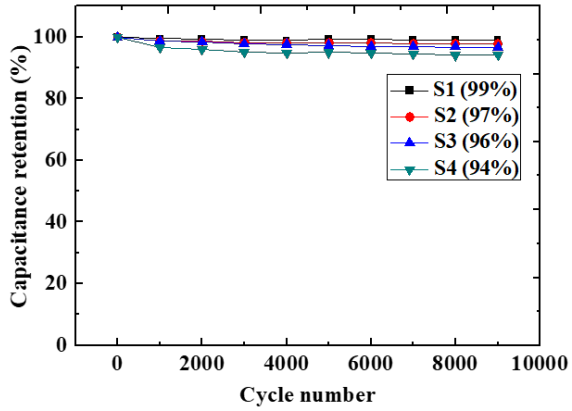

Figure 4. Cycling stability tested at applied current of 35 mA (17.5 A g−1 current density).

Table 2. Specific gravimetric capacitance (C_{sp}) of graphene electrode with different PTFE binder ratios.

Sample	Ratio of PTFE Binder (wt.%)	C_{sp} (F g^{-1})	Capacitance retention at 10,000 cycles
S1	1	74.87	99 %
S2	5	102.75	97%
S3	10	135.88	96%
S4	15	CV: 313.95 GCD: 373.00	94%

Although 15 wt. % PTFE binder in graphene electrode exhibits excellent capacitive performance based on CV and GCD testing, their capacitance retention is lower compared to the other ratios of electrode materials. The findings demonstrate that there is no intrinsic difference between various ratios throughout the study of the long cycle. However, there was a very minor difference from the outcome. This can be ascribed to the electrolyte and binder decomposition at 0.5 to 1.0 V [30]. Also, one can anticipate that the physicochemical features of the carbon material and the electrolyte's composition may affect the production of oxygenated functionalities on the surface of the graphene-PTFE electrode, the change in porosity by the binder, and the ion diffusion in the pores [31]. These two factors should affect its long-cycle performance.

Hence, these findings demonstrate that supercapacitors' capacitance performance and cycling stability may vary depending on the PTFE ratio. In major cases, the electrochemical properties are determined by active materials such as graphene and not the binder material. Binder is a material that determines the adhesion of electrodes, not the capacitance. However, in this work, it can be suggested that the strength of adhesion of active material to the current collector allows

the electrons to flow smoothly. In addition to that, it is strongly believed that the binder ratio exceeding or more than 15 wt. % is considered too much insulative to bind the slurry and the current collector.

CONCLUSION

In conclusion, the low-cost slurry technique is proven to be a feasible process for preparing graphene electrodes for high-performance ultracapacitor/supercapacitor applications. The electrochemical properties are observed to be highly dependent on the type and volume of the binder material. During the CV analyses, as the PTFE binder ratio rises from 1 to 15 wt. %, the as-prepared graphene electrode possesses the highest specific capacitance of 313.95 F g^{-1} (15 wt. %), followed by 135.88 F g^{-1} (10 wt. %), 102.75 F g^{-1} (5 wt. %), and 74.87 F g^{-1} (1 wt. %) at 1 mV s^{-1}. And from the GCD, the specific gravimetric capacitance was calculated to be 373 F g^{-1}. In addition, the fabricated graphene electrode represented cyclic stability with capacitance retention of S1, S2, S3, and S4 are decreasing consistently from 99 to 94 %. These graphene electrodes may work well in applications like consumer electronics and hybrid electric cars due to their overall high performance. These findings demonstrate that an electrode made of graphene and PTFE has the potential for use in high-performance supercapacitors.

ACKNOWLEDGEMENT

The authors acknowledge the Universiti Teknikal Malaysia Melaka for the facilities support and also thankful to the Ministry of Higher Education, Malaysia, for the financial support under a project numbered LRGS15-003-0004.

REFERENCES

[1] L. Feng, Y. Zhu, H. Ding, and C. Ni, "Recent progress in nickel based materials for high performance pseudocapacitor electrodes," *J. Power Sources*, vol. 267, pp. 430-444, 2014, doi: 10.1016/j.jpowsour.2014.05.092.

[2] R. N. A. R. Seman, M. A. Azam, and M. H. Ani, "Graphene/transition metal dichalcogenides hybrid supercapacitor electrode: status, challenges, and perspectives," *Nanotechnology*, vol. 29, pp. 502001, 2018, doi: 10.1088/1361-6528/aae3da.

[3] M.B. Hanif, M. Motola, S. Rauf, C.J. Li, and C.X. Li, "Recent advancements, doping strategies and the future perspective of perovskite-based solid oxide fuel cells for energy conversion," *Chem. Eng. J.*, vol. 428, pp.132603, 2022, doi: 10.1016/j.cej.2021.132603.

[4] V. Ganesh, S. Pitchumani, and V. Lakshminarayanan, "New symmetric and asymmetric supercapacitors based on high surface area porous nickel and activated carbon," *J. Power Sources*, vol. 158, pp. 1523-1532, 2016, doi: 10.1016/j.jpowsour.2005.10.090.

[5] R. N. A. R. Seman, M. A. Azam, and A. A. Mohamad, "Systematic gap analysis of carbon nanotube-based lithium-ion batteries and electrochemical capacitors," *Renew. Sust. Energ. Rev.*, vol. 75, pp. 644-659, 2017, doi: 10.1016/j.rser.2016.10.078.

[6] M. A. Azam, E. Talib, and R. N.A .R .Seman, "Direct deposition of multi-walled carbon nanotubes onto stainless steel and YEF foils using a simple electrophoretic deposition for electrochemical capacitor electrode," *Mater. Res. Express*, vol. 6, no. 1, pp. 015501, 2019, doi: 10.1088/2053-1591/aae293.

[7] A. Afif, S.M. Rahman, A. T. Azad, J. Zaini, M. A. Islan, and A. K. Azad, "Advanced materials and technologies for hybrid supercapacitors for energy storage–a review," *J. Energy Storage*, vol. 25, pp. 100852, 2019, doi: 10.1016/j.est.2019.100852.

[8] Z. Yang, J. Tian, Z. Yin, C. Cui, W. Qian, and F. Wei, :Carbon nanotube-and graphene-based nanomaterials and applications in high-voltage supercapacitor: A review," *Carbon*, vol. 141, pp. 467-480, 2019, doi: 10.1016/j.carbon.2018.10.010.

[9] D. D. Babu, M. Mathew, and S. Thomas, "Supercapacitors based on MXenes (transition metal carbides and nitrides) and their hybrids," in *Fundamentals and Supercapacitor Applications of 2D Materials*, pp. 217-233, 2021, doi: 10.1016/B978-0-12-821993-5.00006-6.

[10] Z. Zhu *et al.*, "Effects of various binders on supercapacitor performances," *Int. J. Electrochem. Sci.*, vol. 11, pp. 8270-8279, 2016, doi: 10.20964/2016.10.04.

[11] D. G. Gromadskyi, J. H. Chae, S. A Norman, and G. Z. Chen, "Correlation of energy storage performance of supercapacitor with iso-propanol improved wettability of aqueous electrolyte on activated carbon electrodes of various apparent densities," *Appl. Energy*, vol. 159, pp. 39-50, 2015, doi: 10.1016/j.apenergy.2015.08.108.

[12] H. Lee, H. Kim, M. S. Cho, J. Choi, and Y. Lee, "Fabrication of polypyrrole (PPy)/carbon nanotube (CNT) composite electrode on ceramic fabric for supercapacitor applications," *Electrochim. Acta*, vol. 56, pp. 7460-7466, 2011, doi: 10.1016/j.electacta.2011.06.113.

[13] F. Tao, Y. Q. Zhao, G. Q. Zhang, and H. L. Li, "Electrochemical characterization on cobalt sulfide for electrochemical supercapacitors," *Electrochem. Commun.*, vol. 9, pp. 1282-1287, 2007, doi: 10.1016/j.elecom.2006.11.022.

[14] S. Cheng, and J. Wu, "Air-cathode preparation with activated carbon as catalyst, PTFE as binder and nickel foam as current collector for microbial fuel cells," *Bioelectrochemistry*, vol. 92, pp. 22-26, 2013, doi: 10.1016/j.bioelechem.2013.03.001.

[15] S. Zhong, C. Zhan, and D. Cao, "Zeolitic imidazolate framework-derived nitrogen-doped porous carbons as high performance supercapacitor electrode materials," *Carbon*, vol. 85, pp. 51-59, 2015, doi: 10.1016/j.carbon.2014.12.064.

[16] P. F. R. Ortega, J. P. C. Trigueiro, G. G. Silva, and R. L. Lavall, Improving supercapacitor capacitance by using a novel gel nanocomposite polymer electrolyte based on nanostructured SiO2, PVDF and imidazolium ionic liquid," *Electrochim. Acta*, vol. 188, pp. 809-817, 2016, doi: 10.1016/j.electacta.2015.12.056.

[17] R. Singh, S. Janakiraman, M. Khalifa, S. Anandhan, S. Ghosh, A. Venimadhav, and K. Biswas, "An electroactive β-phase polyvinylidene fluoride as gel polymer electrolyte for magnesium–ion battery application," *J. Electroanal. Chem.*, vol. 851, pp. 113417, 2019, doi: 10.1016/j.jelechem.2019.113417.

[18] M. A. Azam, M.A. Azam, N.E. Safie, M.F.A. Aziz, et al., "Structural characterization and electrochemical performance of nitrogen doped graphene supercapacitor electrode fabricated by hydrothermal method," *International Journal of Nanoelectronics and Materials*, vol. 14, ni. 2, pp. 127-136, 2021.

[19] M.A. Azam *et al.*, "Direct observation of graphene during Raman analysis and the effect of precursor solution parameter on the graphene structures," *Diamond and Related Materials*, vol. 104, pp. 107767, 2020, doi: 10.1016/j.diamond.2020.107767.
[20] Y. Wang *et al.*, "Supercapacitor devices based on graphene materials," *J. Phys. Chem. C*, vol. 113, pp. 13103-13107, 2009, doi: 10.1021/jp902214f.
[21] K. C. Pham, D. S. McPhail, A. T. S. Wee, and D. H. C. Chua, "Amorphous molybdenum sulfide on graphene–carbon nanotube hybrids as supercapacitor electrode materials," *RSC Adv.*, vol. 7, pp. 6856-6864, 2017, doi: 10.1039/C6RA27901E.
[22] R. N. A. R. Seman, and M. A. Azam, "Hybrid heterostructures of graphene and molybdenum disulfide: the structural characterization and its supercapacitive performance in 6M KOH electrolyte," J. *Sci.: Adv. Mater. Devices*, vol. 5, pp. 554-559, 2020, doi: 10.1016/j.jsamd.2020.09.010.
[23] H. I. Maarof, W. M. A. W. Daud, and M. K. Aroua, "Effect of varying the amount of binder on the electrochemical characteristics of palm shell activated carbon," *IOP Conf. Ser.: Mater. Sci. Eng.*, vol. 210, pp. 012011, 2017, doi: 10.1088/1757-899X/210/1/012011.
[24] A. Y. Lo, L. Saravanan, C. M. Tseng, F. K. Wang, and J. T. Huang, " Effect of composition ratios on the performance of graphene/ carbon nanotube/manganese oxide composites toward supercapacitor applications," *ACS OMega*, vol. 5, pp. 578-587, 2020, doi: 10.1021/acsomega.9b03163.
[25] Y. Guo *et al.*, "One-pot synthesis of graphene/zinc oxide by microwave irradiation with enhanced supercapacitor performance," *RSC Adv.*, vol. 6, pp. 19394-19403, 2016, doi: 10.1039/C5RA24212F.
[26] N. An *et al.*, "Hierarchical porous covalent organic framework/graphene aerogel electrode for high-performance supercapacitors," *J. Mater. Chem. A*, vol. 9 pp. 16824-16833, 2021, doi: 10.1039/D1TA04313G.
[27] G. Xiong, P. He, D. Wang, Q. Zhang, T. Chen, and T. S. Fisher, "Hierarchical Ni–Co hydroxide petals on mechanically robust graphene petal foam for high-energy asymmetric supercapacitors," *Adv. Funct. Mater.*, vol. 26, pp. 1-11, 2016, doi: 10.1002/adfm.201600879.
[28] R. N. A. R. Seman, M. A. Azam, and M. A. Mohamed, "Highly efficient growth of vertically aligned carbon nanotubes on Fe–Ni based metal alloy foils for supercapacitors," *Adv. Nat. Sci: Nanosci. Nanotechnol.*, vol. 7, pp. 045016, 2016, doi: 10.1088/2043-6262/7/4/045016.
[29] B. Xie *et al.*, "Hydrothermal synthesis of layered molybdenum sulfide/N-doped graphene hybrid with enhanced supercapacitor performance," *Carbon*, vol. 99, pp. 35-42, 2016, doi: 10.1016/j.carbon.2015.11.077.
[30] H. Y. Tran, M. Wohlfahrt-Mehrens, and S. Dsoke, "Influence of the binder nature on the performance and cycle life of activated carbon electrodes in electrolytes containing Li-salt," *J. Power Sources*, vol. 342, pp. 301-312, 2017, doi: 10.1016/j.jpowsour.2016.12.056.
[31] Q. Abbas, D. Pajak, E. Frąckowiak, and F. Béguin, "Effect of binder on the performance of carbon/carbon symmetric capacitors in salt aqueous electrolyte," *Electrochim. Acta*, vol. 140, pp. 132-138, 2014, doi: 10.1016/j.electacta.2014.04.096.